



RESEARCH ARTICLE

# Structural considerations for charge-enhanced Brønsted acid catalysts

Curtis Payne  | Steven R. Kass 

Department of Chemistry, University of Minnesota, Minneapolis, MN, USA

## Correspondence

Steven R. Kass, Department of Chemistry, University of Minnesota, 207 Pleasant Street SE, Minneapolis, Minnesota 55455, USA.  
Email: kass@umn.edu

## Funding information

National Science Foundation, Grant/Award Number: CHE-1665392

## Abstract

All three *N*-methylated and *N*-protonated hydroxypyridinium  $\text{BAr}_4^{\text{F}}^-$  salt isomers were synthesized and their hydrogen bond donating abilities were investigated. DFT and G4 theory computations along with IR spectroscopic measurements were found to be effective methods for predicting the catalytic activities of these O–H and N–H Brønsted acids. A UV-vis titration approach for rapidly quantifying hydrogen bond donating ability revealed that carbon-hydrogen bonds also can participate in electrostatic interactions, but the presence of multiple equilibrium complexes results in a limitation of this method. In the methylated series of hydroxypyridines, the ortho and para isomers displayed modest rate enhancements relative to the meta derivative. Protonation introduces a new acidic site and the ortho hydroxypyridinium ion salt is a significantly more active catalyst than all of the other species examined. This is indicative of bidentate activation by the N–H and O–H acidic sites, and suggests a new design strategy for improving charge-enhanced catalysts.

## KEYWORDS

Brønsted acid catalysis, charge-activated acids, computations, IR and UV-vis spectroscopy, kinetics

## 1 | INTRODUCTION

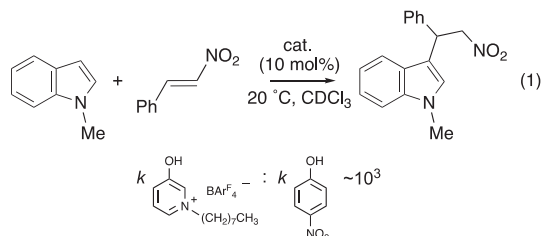
Enzymes exploit hydrogen bonds to control their three-dimensional structures, facilitate substrate molecular recognition and binding, and accelerate reaction processes.<sup>[1]</sup> Their catalytic ability is intertwined with numerous chemical mechanisms, but often involves electrophilic activation of a substrate toward nucleophilic attack by lowering the energy of its lowest unoccupied molecular orbital (LUMO).<sup>[2]</sup> As a result, the development of small metal-free Brønsted acids and hydrogen bond donors to catalyze a wealth of organic transformations has emerged as an attractive research area in the past several decades.<sup>[3]</sup> From these studies it has been found that for the same class of compounds with the same binding motifs, that the acidity of the catalyst often correlates with its activity.<sup>[4]</sup> It is for this reason that

electron-withdrawing substituents are commonly employed to improve reactivity.<sup>[5]</sup> For example, phenyl rings are routinely replaced by bis(3,5-trifluoromethyl) phenyl groups, and this latter framework is viewed as occupying a privileged position.<sup>[6]</sup>

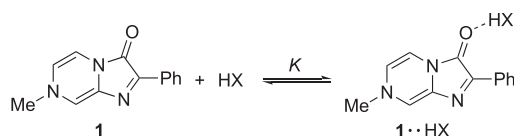
Brønsted acids are routinely characterized by their  $\text{p}K_{\text{a}}$  values which typically are measured in water, dimethyl sulfoxide, or acetonitrile.<sup>[7]</sup> These solvents have high dielectric constants which facilitate the acidity determinations and lead to solvent separated ion pairs. Brønsted acids and hydrogen bond donating organocatalysts, however, are usually employed in non-polar media such as toluene, chloroform, and dichloromethane where intimate ion pairs and aggregates are formed. Substituent effects and catalyst activities, consequently may be poorly represented by routinely determined  $\text{p}K_{\text{a}}$  values. To address this issue, Kozłowski

et al. developed a UV-vis spectroscopy approach in which a colorimetric sensor, 7-methyl-2-phenylimidazo[1,2-a]pyrazine-3(7H)-one (**1**) is titrated with a hydrogen bond donor (HX) in dichloromethane (Scheme 1).<sup>[8]</sup> The reciprocals of the observed blue-shifts of the bound complexes (**1**•HX) were found to correlate with the logarithms of the association binding constants ( $K$ ) and the rate constants ( $k$ ) for the Diels Alder reaction of cyclopentadiene with methyl vinyl ketone.

More recently, we made use of IR spectroscopy to determine the relative acidities of substituted phenols in carbon tetrachloride by examining the change in their O–H stretching frequencies ( $\Delta\nu$ ) upon addition of a small amount of a hydrogen bond acceptor (i.e., CD<sub>3</sub>CN).<sup>[9]</sup> It was found that  $\Delta\nu$  correlates with the gas-phase acidity more strongly than DMSO  $pK_a$  values. This led to the suggestion and observation that charged substituents are much more effective at enhancing acidities and catalytic abilities than neutral polar groups such as CF<sub>3</sub>, CN, and NO<sub>2</sub>. For example, it was found that the Friedel-Crafts reaction between *N*-methylindole and *trans*- $\beta$ -nitrostyrene in chloroform occurs  $\sim 10^3$  times more rapidly when *N*-octyl-3-hydroxypyridinium tetrakis[3,5-bis(trifluoromethyl)phenyl]borate (BAr<sup>F</sup><sub>4</sub>) rather than when 4-nitrophenol is used as the catalyst (equation 1).



Since this discovery, achiral and chiral thioureas<sup>[10]</sup> and phosphoric acids<sup>[11]</sup> have been investigated with this charge-activated design. In these reports, the charged center was introduced most commonly with a 3-substituted *N*-alkylated pyridine ring.<sup>[12]</sup> Other cationic compounds such as amidinium,<sup>[13]</sup> guanidinium,<sup>[14]</sup> ammonium,<sup>[15]</sup> pyridinium,<sup>[16]</sup> and quinolinium<sup>[17]</sup> ions also have been shown to accelerate a variety of chemical transformations.<sup>[18]</sup> These protonated compounds are more acidic than their neutral conjugate bases and have an additional hydrogen bond donating site that can alter the binding motif of the catalyst, and enhance its association with the substrate. To address the impact of the



**SCHEME 1** UV-vis sensor **1** and its bound complex with a Brønsted acid

structural framework on catalyst activity, we report herein on all three isomers of *N*-methylated and *N*-protonated hydroxypyridinium BAr<sup>F</sup><sub>4</sub><sup>−</sup> salts along with the two parent pyridinium ions (Figure 1). These compounds were probed by IR and UV-vis spectroscopy, DFT and G4 theory computations,<sup>[19]</sup> and a pseudo-first-order rate study.

## 2 | EXPERIMENTAL

### 2.1 | General

All reaction glassware (vials, NMR tubes, flasks) and stir bars were dried in an oven (120°C) for at least 16 h, and glass syringes and volumetric flasks were stored in a vacuum desiccator over Drierite for at least 16 h. Alumina (neutral, Brockman I, standard grade, 150 mesh, 58 Å) and 3 Å molecular sieves were activated at 300°C for at least 24 h. Calcium chloride was obtained from Fischer Scientific and was dried at 300°C for at least 30 min (note: after 24 h at this temperature, the CaCl<sub>2</sub> becomes tan and the use of this discolored material led to poor results).

Anhydrous acetonitrile and iodomethane were obtained from Acros Organics and used without further purification. 1,2-Dichloroethane (DCE) was purchased from Fischer Scientific and was dried with a column of activated alumina and stored over 3 Å molecular sieves under inert atmosphere for at least 24 h prior to use. *N*-Methylindole was used as received from Alfa Aesar. Concentrated HCl (37%) was obtained from VWR International. Sodium tetrakis(3,5-bis(trifluoromethyl)phenyl)borate (NaBAr<sup>F</sup><sub>4</sub>) was obtained as a 2.5 hydrate (based on its <sup>1</sup>H NMR spectrum) from AK Scientific. The water was removed by dissolving the material in anhydrous methanol (2 g in 2 mL) and running the light-yellow mixture through two pipets of activated alumina (1.25 g/pipet, each pipet was rinsed with an additional 2 mL of methanol) and then through a 0.45 μm syringe filter. The solvent was removed with a rotary evaporator and the remaining colorless solid was ground into a fine powder and heated at 150°C at 0.1 torr for at least 16 h<sup>[20]</sup> in a glovebox (less than 0.06 H<sub>2</sub>O remained based upon the <sup>1</sup>H NMR spectrum). *N*-Methyl-2-pyridone was acquired

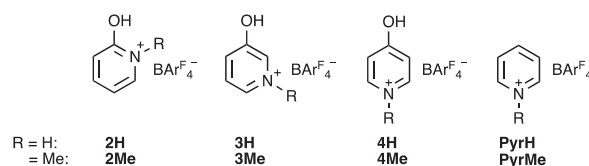


**FIGURE 1** Charged catalysts screened in this work

from ArkPharm, Inc. as a dark brown oil that was dissolved in anhydrous ethyl acetate, passed through a column of activated alumina (1.25 g), and concentrated to afford a light-yellow oil. In a similar manner, 2-methoxypyridine (Oakwood Chemical) was dried with an activated alumina column in anhydrous  $\text{CH}_2\text{Cl}_2$ .

All other chemicals and anhydrous solvents were supplied by Sigma-Aldrich and were used as received unless described below. Pentane was stored over 3 Å molecular sieves under argon for 24 h prior to use. Pyridine was dried with a short column of activated alumina and stored over 3 Å molecular sieves under inert atmosphere for 2 days prior to use.<sup>[21]</sup> 2- and 3-Hydroxypyridines were dried by dissolving 300 mg samples in 2 mL of anhydrous methanol and passing the yellow mixture through a Pasteur pipet  $\frac{3}{4}$  full of activated alumina (~1.25 g). After rinsing the column with additional solvent (2 mL), the colorless solution was concentrated with a rotary evaporator and then a mechanical pump (0.1 torr), and the remaining white solid was stored in a glovebox. 4-Hydroxypyridine was dried in a similar manner to its isomers but was melted at 150°C while under reduced pressure (0.1 torr) for 5 min to remove any residual water (30 min under these conditions led to discoloration and presumed decomposition).

Deuterated solvents came from Cambridge Isotope Laboratories and were stored over 3 Å molecular sieves for at least 24 h prior to use. Bruker Avance III HD 400 or 500 MHz instruments were used to collect  $^1\text{H}$ ,  $^{13}\text{C}$ , and  $^{19}\text{F}$  NMR spectra. All chemical shifts are reported in ppm ( $\delta$ ) and  $^1\text{H}$  and  $^{13}\text{C}$  spectral data are referenced as follows:  $\delta$  5.32 and 54.0 ( $\text{CD}_2\text{Cl}_2$ ); 1.94 and 118.3 ( $\text{CD}_3\text{CN}$ ); 2.50 and 39.5 ( $d_6$ -DMSO). Fluorobenzene was used as an internal standard for all  $^{19}\text{F}$  spectra ( $\delta$  -113.78 in  $\text{CD}_2\text{Cl}_2$ ; -114.81 in  $\text{CD}_3\text{CN}$ ).<sup>[22]</sup>

Thin layer chromatography was carried out with Macherey-Nagel precoated polyester sheets (0.2 mm alumina with a fluorescent indicator) and visualized using a UV lamp. Purification by MPLC was carried out with a CombiFlash®  $R_f$  automated flash chromatography system from Teledyne Isco, Inc. on alumina (neutral, Brockman I, standard grade, 150 mesh, 58 Å) columns. Uncorrected melting points were observed with a Thomas Hoover Uni-Melt apparatus in unsealed capillaries. FT-IR data for characterization were collected with a Thermo Scientific Nicolet iS5 spectrometer with an iD5 ATR source and solution measurements were observed with a liquid cell (1.0 mm path length) with NaCl windows. In all cases, ~5 mM phenol solutions were made in both dry  $\text{CD}_2\text{Cl}_2$  and dry 1%  $\text{CD}_3\text{CN}/\text{CD}_2\text{Cl}_2$  (v:v).<sup>[9]</sup> Backgrounds of the solvent mixtures were used to correct the corresponding spectra. Between each run, the cell was rinsed with  $\text{CH}_2\text{Cl}_2$  and then purged with a flow of

$\text{N}_2$  for 10 min. High resolution electrospray ionization mass spectra (HRMS-ESI) were obtained in methanol with a Bruker ESI-BioTOF instrument, and tetramethylammonium and tetraethylammonium salts were used as mass calibrants. Due to the low masses of the protonated salts (~96 m/z), protonated 2,6-lutidine was used as a third calibration point. UV spectra were collected with a Lambda XLS spectrometer from  $\text{CH}_2\text{Cl}_2$  solutions in a 10 mm quartz cell that was sealed with a PTFE septum.

### 2.1.1 | *N*-Methyl-4-pyridone<sup>[23]</sup>

In a 25 mL round-bottomed flask fitted with a reflux condenser, 4-hydroxypyridine (200 mg, 2.10 mmol) and toluene (5 mL) were stirred and the atmosphere was purged with argon for 15 min. Iodomethane (700  $\mu\text{L}$ , 1.60 g, 11.2 mmol) was then added in one portion by syringe and the resulting mixture was refluxed overnight. Upon cooling to room temperature an orange precipitate and a light-yellow supernatant remained. Hexanes (15 mL) were added to the suspension and the solid was isolated via vacuum filtration. The collected material (~460 mg) was placed in a 6-dram vial, dissolved in methanol (5 mL), and  $\text{K}_2\text{CO}_3$  (300 mg, 2.17 mmol) was added with vigorous stirring. After 2 h the reaction mixture was filtered, and the solid material was rinsed with 5 mL of methanol. Removal of the solvent under reduced pressure afforded a yellow oily solid which was dissolved in 5 mL of  $\text{CH}_2\text{Cl}_2$ . A white precipitate was filtered away and the light-yellow filtrate was concentrated with a rotary evaporator to give 146 mg of an oily solid. Purification of this material by column chromatography on alumina with 95/5 MeOH/ $\text{CH}_2\text{Cl}_2$  ( $R_f$  = 0.3) afforded 104 mg (45%) of a colorless powder (mp 93 – 96°C) that was stored in a glovebox.  $^1\text{H}$  NMR (500 MHz,  $\text{CD}_2\text{Cl}_2$ )  $\delta$  7.23 (d,  $J$  = 7.2 Hz, 2H), 6.20 (d,  $J$  = 7.3 Hz, 2H), 3.58 (s, 3H).  $^{13}\text{C}$  NMR (125 MHz,  $\text{CD}_2\text{Cl}_2$ )  $\delta$  178.5, 141.1, 118.8, 43.9. IR (ATR source) 1674, 1637, 1555  $\text{cm}^{-1}$ .

### 2.1.2 | *N*-Methyl-3-hydroxypyridinium iodide

In a 25 mL round-bottomed flask fitted with a reflux condenser, 3-hydroxypyridine (300 mg, 3.15 mmol) and acetonitrile (6 mL) were stirred and the atmosphere was purged with argon for 10 min. Iodomethane (200  $\mu\text{L}$ , 456 mg, 3.21 mmol) was rapidly added and the resulting solution was refluxed overnight. Upon cooling to room temperature, the reaction mixture was concentrated with

a rotary evaporator and subsequently dissolved in 1 mL of anhydrous methanol. Dropwise addition of the yellow material into 20 mL of anhydrous ethyl acetate in a 6-dram vial with vigorous stirring under an inert atmosphere afforded a white precipitate. The yellow supernatant was removed via syringe and the solid residue was washed with ethyl acetate in 10 mL portions until the solvent became colorless. A rotary evaporator followed by a mechanical pump (0.1 torr) were used to dry the product and 668 mg (89%) of an off-white fluffy solid (mp 112 – 113°C) was obtained. This material was stored in a glovebox.  $^1\text{H}$  NMR (500 MHz,  $\text{CD}_3\text{CN}$ )  $\delta$  9.64 (OH, s, 1H), 8.50 (s, 1H), 8.24–8.23 (m, 2H), 7.81 (t,  $J$  = 7.8 Hz, 1H), 4.25 (s, 3H).  $^{13}\text{C}$  NMR (125 MHz,  $\text{CD}_3\text{CN}$ )  $\delta$  157.6, 137.7, 134.7, 132.6, 129.2, 49.4. IR (ATR source) 2963, 1581, 1506, 1492  $\text{cm}^{-1}$ . HRMS-ESI: calcd for  $\text{C}_6\text{H}_8\text{NO}$  ( $\text{M} - \text{I}^+$ ) $^+$  110.0606, found 110.0586.

### 2.1.3 | *N*-Methyl-3-hydroxypyridinium tetrakis(3,5-bis (trifluoromethyl)phenyl) borate (3Me)

In a 6-dram vial under argon, *N*-methyl-3-hydroxypyridinium iodide (31.9 mg, 0.135 mmol) and sodium tetrakis(3,5-bis (trifluoromethyl)phenyl)borate (132 mg, 0.148 mmol) were added to 3 mL of anhydrous  $\text{CH}_2\text{Cl}_2$  and vigorously stirred overnight. A white precipitate was filtered with a 0.45  $\mu\text{m}$  syringe filter and then washed with 2 mL of additional  $\text{CH}_2\text{Cl}_2$ . The combined liquid material was concentrated with a rotary evaporator and the resulting solid residue was dissolved in 2 mL of  $\text{CH}_2\text{Cl}_2$ . This solution was added dropwise to 15 mL of anhydrous pentane in a 6-dram vial with stirring. A white solid formed immediately and was allowed to settle to the bottom of the vial before the supernatant was removed via syringe. The solid product was resuspended in 15 mL of pentane, collected by vacuum filtration, and washed with 15 mL of pentane. It was then dissolved in 4 mL of  $\text{CH}_2\text{Cl}_2$ , dried over  $\text{MgSO}_4$ , and concentrated under reduced pressure to afford 82.6 mg (63%) of a white solid (mp 179 – 180°C).  $^1\text{H}$  NMR (500 MHz,  $\text{CD}_2\text{Cl}_2$ )  $\delta$  8.05 (s, 1H), 8.01 (d,  $J$  = 8.0 Hz, 1H), 7.89 (d,  $J$  = 7.9 Hz, 1H), 7.81–7.80 (m, 1H), 7.76 (s, 8H), 7.59 (s, 4H) 6.39 (OH, s, 1H), 4.26 (s, 3H).  $^{13}\text{C}$  NMR (125 MHz,  $d_6$ -DMSO)  $\delta$  161.0 (q,  $^1J_{\text{B-C}}$  = 50.0 Hz), 156.7, 136.4, 134.1, 133.8, 130.9, 128.5 (qq,  $^3J_{\text{B-C}}$  = 2.7 Hz and  $^2J_{\text{F-C}}$  = 31.6 Hz), 128.3, 124.0 (q,  $^1J_{\text{F-C}}$  = 273 Hz), 117.7 (sept,  $^3J_{\text{F-C}}$  = 4.1 Hz),<sup>[24]</sup> 47.8.  $^{19}\text{F}$  (376 MHz,  $\text{CD}_2\text{Cl}_2$ )  $\delta$  -62.6. IR (ATR source) 3593, 3510, 1611, 1598, 1516, 1354, 1275, 1104  $\text{cm}^{-1}$ . HRMS-ESI: calcd for  $\text{C}_6\text{H}_8\text{NO}$  ( $\text{M} - \text{C}_{32}\text{H}_{12}\text{BF}_{24}$ ) $^+$  110.0606, found 110.0583.

### 2.1.4 | *N*-Methyl-2-hydroxypyridinium trifluoromethanesulfonate<sup>[25]</sup>

In a 6-dram vial under inert atmosphere, *N*-methyl-2-pyridone (100  $\mu\text{L}$ , 111 mg, 1.02 mmol) was dissolved in 1 mL of anhydrous  $\text{CH}_2\text{Cl}_2$ . Neat trifluoromethanesulfonic acid (90  $\mu\text{L}$ , 153 mg, 1.02 mmol) was then added dropwise over 2–3 min at room temperature. A white precipitate was observed after 10 min and the suspension was stirred for a total of 1 h. The reaction mixture was diluted with 10 mL of pentane and the supernatant was removed via syringe. The solid residue was washed twice with 10 mL of pentane, and then dried with a rotary evaporator followed by a mechanical pump to afford 252 mg (95%) of a shiny, colorless solid (mp 109 – 110°C) that was stored in a glovebox.  $^1\text{H}$  NMR (500 MHz,  $\text{CD}_3\text{CN}$ )  $\delta$  12.05 (bs, OH, 1H), 8.20 (t,  $J$  = 8.1 Hz, 1H), 8.12 (d,  $J$  = 6.6 Hz, 1H), 7.43 (d,  $J$  = 8.7 Hz, 1H), 7.29 (t,  $J$  = 6.9 Hz, 1H), 3.91 (s, 3H).  $^{13}\text{C}$  NMR (125 MHz,  $\text{CD}_3\text{CN}$ )  $\delta$  161.1, 147.9, 143.2, 121.5 (q,  $^1J_{\text{F-C}}$  = 319 Hz), 118.7, 115.3, 41.6.  $^{19}\text{F}$  (376 MHz,  $\text{CD}_3\text{CN}$ )  $\delta$  -79.4. IR (ATR source) 2932, 1644, 1601, 1520, 1287, 1217, 1156, 1023  $\text{cm}^{-1}$ . HRMS-ESI: calcd for  $\text{C}_6\text{H}_8\text{NO}$  ( $\text{M} - \text{CF}_3\text{SO}_3$ ) $^+$  110.0606, found 110.0581.

### 2.1.5 | *N*-Methyl-2-hydroxypyridinium tetrakis(3,5-bis (trifluoromethyl)phenyl) borate (2Me)

In a 6-dram vial, *N*-methyl-2-hydroxypyridinium trifluoromethanesulfonate (25.9 mg, 0.100 mmol) and sodium tetrakis(3,5-bis(trifluoromethyl)phenyl)borate (99.9 mg, 0.113 mmol) were added and the atmosphere was purged with argon. Anhydrous  $\text{CH}_2\text{Cl}_2$  (3 mL) was then added and the resulting suspension was vigorously stirred for 5.5 h. The reaction mixture was filtered through a 0.45  $\mu\text{m}$  syringe filter and then washed with 2 mL of additional  $\text{CH}_2\text{Cl}_2$ . The solvent was removed with a rotary evaporator and the solid residue was dissolved in 1 mL of  $\text{CH}_2\text{Cl}_2$  and the filtration procedure was repeated. Further drying was performed with a mechanical pump to afford 96.2 mg (99%) of a colorless solid (mp 105 – 106°C).  $^1\text{H}$  NMR (500 MHz,  $\text{CD}_2\text{Cl}_2$ )  $\delta$  11.62 (bs, OH, 1H), 8.15 (dt,  $J$  = 8.1 and 1.4 Hz, 1H), 7.93 (dd,  $J$  = 6.6 and 1.3 Hz, 1H), 7.73 (s, 8H), 7.56 (s, 4H), 7.28 (m, 2H), 3.97 (s, 3H).  $^{13}\text{C}$  NMR (125 MHz,  $\text{CD}_2\text{Cl}_2$ )  $\delta$  162.3 (q,  $^1J_{\text{B-C}}$  = 49.5 Hz), 161.0, 147.6, 141.6, 135.4, 129.5 (qq,  $^3J_{\text{B-C}}$  = 2.7 Hz and  $^2J_{\text{F-C}}$  = 31.6 Hz), 125.2 (q,  $^1J_{\text{F-C}}$  = 273 Hz), 118.4, 118.1 (sept,  $^3J_{\text{F-C}}$  = 4.1 Hz),<sup>[26]</sup> 115.5, 41.7.  $^{19}\text{F}$  (376 MHz,  $\text{CD}_2\text{Cl}_2$ )  $\delta$  -62.7. IR (ATR source) 3695, 3617, 1646, 1606, 1521, 1353, 1273, 1105  $\text{cm}^{-1}$ .



HRMS-ESI: calcd for  $C_6H_8NO$  ( $M - C_{32}H_{12}BF_{24}^-$ )<sup>+</sup> 110.0606, found 110.0587.

### 2.1.6 | 4-Hydroxypyridinium trifluoromethanesulfonate

In a 6-dram vial, 4-hydroxypyridine (52.5 mg, 0.552 mmol) was suspended in 1 mL of anhydrous acetonitrile and the atmosphere was purged with argon for 15 min. Neat trifluoromethanesulfonic acid (100  $\mu$ L, 170 mg, 1.13 mmol) was then added dropwise over 2–3 min at room temperature resulting in a colorless clear solution that was stirred for an additional 30 min. The reaction mixture was diluted with 10 mL of anhydrous diethyl ether and then 10 mL of pentane was added to form a white precipitate. The supernatant was removed by syringe and the solid residue was washed twice with 10 mL of pentane. The product was dried on a rotary evaporator followed by a mechanical pump at 110°C for 4 h to afford 101 mg (75%) of a light tan solid (mp 111 – 113°C) which was stored in a glovebox. <sup>1</sup>H NMR (500 MHz, CD<sub>3</sub>CN)  $\delta$  12.30 (bt, NH,  $J_{N-H}$  = 56.0 Hz, 1H), 10.78 (bs, OH, 1H), 8.39 (d,  $J$  = 7.3 Hz, 2H), 7.31 (d,  $J$  = 7.5 Hz, 2H). <sup>13</sup>C NMR (125 MHz, CD<sub>3</sub>CN)  $\delta$  172.8, 143.7, 121.6 (q,  $^1J_{F-C}$  = 319 Hz), 115.1. <sup>19</sup>F (376 MHz, CD<sub>3</sub>CN)  $\delta$  -79.4. IR (ATR source) 3245, 3101, 1648, 1612, 1513, 1271, 1249, 1211, 1190, 1171, 1024 cm<sup>-1</sup>. HRMS-ESI: calcd for  $C_5H_6NO$  ( $M - CF_3SO_3^-$ )<sup>+</sup> 96.0449, found 96.0437.

### 2.1.7 | 4-Hydroxypyridinium tetrakis(3,5-bis (trifluoromethyl)phenyl)borate (4H)

In a 6-dram vial, 4-hydroxypyridinium trifluoromethanesulfonate (20.5 mg, 0.0836 mmol) and sodium tetrakis(3,5-bis (trifluoromethyl)phenyl)borate (85.0 mg, 0.0959 mmol) were added and the atmosphere was purged with argon. Anhydrous CH<sub>2</sub>Cl<sub>2</sub> (2 mL) was then added and the resulting suspension was vigorously stirred for 4.5 h. The reaction mixture was filtered through a 0.45  $\mu$ m syringe filter and then washed with 2 mL of additional CH<sub>2</sub>Cl<sub>2</sub>. The solvent was removed with a rotary evaporator and the solid residue was dissolved in 1 mL of CH<sub>2</sub>Cl<sub>2</sub> and the filtration procedure was repeated. Further drying was performed with a mechanical pump to afford 74.5 mg (93%) of a colorless solid (mp 162 – 164°C). <sup>1</sup>H NMR (500 MHz, CD<sub>2</sub>Cl<sub>2</sub>)  $\delta$  10.82 (t, NH,  $J_{N-H}$  = 68.0 Hz, 1H), 8.35 (t,  $J$  = 6.9 Hz, 2H), 8.26 (bs, OH, 1H), 7.73 (s, 8H), 7.57 (s, 4H), 7.37 (d,  $J$  = 6.4 Hz, 2H). <sup>13</sup>C NMR (125 MHz, CD<sub>2</sub>Cl<sub>2</sub>)  $\delta$  172.4,

162.3 (q,  $^1J_{B-C}$  = 50.3 Hz), 142.7, 135.4, 129.5 (qq,  $^3J_{B-C}$  = 2.5 Hz and  $^2J_{F-C}$  = 31.4 Hz), 125.2 (q,  $^1J_{F-C}$  = 273 Hz), 118.1 (sept,  $^3J_{F-C}$  = 3.8 Hz),<sup>[26]</sup> 116.1. <sup>19</sup>F (376 MHz, CD<sub>2</sub>Cl<sub>2</sub>)  $\delta$  -62.6. IR (ATR source) 3555, 3488, 3403, 1649, 1608, 1519, 1354, 1274, 1114 cm<sup>-1</sup>. HRMS-ESI: calcd for  $C_5H_6NO$  ( $M - C_{32}H_{12}BF_{24}^-$ )<sup>+</sup> 96.0449, found 96.0438.

### 2.1.8 | N-Methylpyridinium iodide

Following a literature procedure,<sup>[27]</sup> pyridine (200  $\mu$ L, 196 mg, 2.48 mmol) was dissolved in 10 mL of acetonitrile under argon in a 25 mL round-bottomed flask equipped with a reflux condenser. Iodomethane (600  $\mu$ L, 1.37 g, 9.64 mmol) was then added by syringe and the reaction mixture refluxed overnight. Upon cooling to room temperature, the yellow solution was concentrated with a rotary evaporator. The remaining solid residue was then dissolved in 3 mL of acetonitrile and added dropwise into stirring anhydrous diethyl ether under argon (15 mL). A white precipitate formed and was allowed to settle to the bottom before removing the yellow supernatant via syringe. The solid was washed with additional diethyl ether until the supernatant was colorless (4  $\times$  10 mL) and then was dried on a rotary evaporator followed by a mechanical pump to afford 545 mg (99%) of a light-yellow solid (mp 108 – 110°C). <sup>1</sup>H NMR (500 MHz, *d*<sub>6</sub>-DMSO)  $\delta$  9.00 (d,  $J$  = 5.4 Hz, 2H), 8.59 (t,  $J$  = 7.8 Hz, 1H), 8.14 (t, 6.7 Hz, 2H), 4.37 (s, 3H). <sup>13</sup>C NMR (125 MHz, *d*<sub>6</sub>-DMSO)  $\delta$  145.5, 145.0, 127.6, 48.0.

### 2.1.9 | N-Methylpyridinium tetrakis(3,5-bis (trifluoromethyl)phenyl)borate (PyrMe)

In a 6-dram vial under argon, *N*-methylpyridinium iodide (31.2 mg, 0.141 mmol) and sodium tetrakis(3,5-bis (trifluoromethyl)phenyl)borate (134 mg, 0.151 mmol) were added to 3 mL of anhydrous CH<sub>2</sub>Cl<sub>2</sub> and vigorously stirred for 1 h. A white precipitate was filtered with a 0.45  $\mu$ m syringe filter and then washed with 2 mL of additional CH<sub>2</sub>Cl<sub>2</sub>. The combined liquid material was concentrated with a rotary evaporator and the resulting solid residue was dissolved in 2 mL of CH<sub>2</sub>Cl<sub>2</sub>, dried over MgSO<sub>4</sub>, and filtered again. Removal of the solvent under reduced pressure afforded 96.2 mg (71%) of a colorless solid (mp 205 – 206°C) that had spectra consistent with a previous report.<sup>[28]</sup> <sup>1</sup>H NMR (400 MHz, CD<sub>2</sub>Cl<sub>2</sub>)  $\delta$  8.52–8.47 (m, 3H), 8.03 (t,  $J$  = 7.0 Hz, 2H), 7.73 (s, 8H), 7.56 (s, 4H), 4.37 (s, 3H). <sup>13</sup>C NMR (125 MHz, CD<sub>2</sub>Cl<sub>2</sub>)  $\delta$

162.4 (q,  $^1J_{\text{B-C}} = 50.0$  Hz), 147.0, 144.8, 135.4, 129.7, 129.5 (qq,  $^3J_{\text{B-C}} = 2.7$  Hz and  $^2J_{\text{F-C}} = 31.6$  Hz), 125.2 (q,  $^1J_{\text{F-C}} = 273$  Hz), 118.1 (sept,  $^3J_{\text{F-C}} = 4.1$  Hz), 49.7.  $^{19}\text{F}$  (376 MHz,  $\text{CD}_2\text{Cl}_2$ )  $\delta$  -62.7.

## 2.2 | Description of HCl gas apparatus<sup>[29]</sup>

A picture of the reaction setup is given in Figure S1. An argon line was connected to the top of an addition funnel (A) where concentrated HCl (1.0 – 2.0 mL) was stored prior to its slow dropwise addition onto  $\text{CaCl}_2$  (1 g for every 1 mL of conc. HCl) in a 3-necked round-bottomed flask (B). A small drying tube containing 0.5 – 1.0 g of additional  $\text{CaCl}_2$  (C) was used to further dry the HCl prior to entering the 6-dram reaction vial (E) via a 4" needle (D) that could be inserted into the reaction medium; bubbling should be visible when an argon flow is applied to the system. The effluent was then passed through a neutralization column (F) filled with NaOH pellets to scavenge any residual HCl. Finally, an oil-containing bubbler (G) was connected to the end of the apparatus and was useful for identifying leaks and establishing suitable HCl flows.

## 2.3 | General one-pot protonation and anion exchange procedure

In a 6-dram vial, the starting pyridine or pyridone (1.0 eq.),  $\text{NaBARF}_4$  (1.0 – 1.2 eq.), and a stir bar were placed. This reaction vessel was connected to the HCl generation apparatus (Figure S1) and the entire system was purged for 5 min with argon. The desired solvent was then introduced and the resulting suspension was stirred for an additional 5 min. Insertion of the 4" needle into the liquid medium (bubbling should be observed) was followed by charging the addition funnel with concentrated HCl and its subsequent slow dropwise addition onto the  $\text{CaCl}_2$ . Bubbling in the 3-necked round-bottomed flask was observed immediately and after 2–3 min, the suspension in the 6-dram vial became less cloudy but did not clear up entirely. Upon completion of the HCl generation (no further bubbling in the 3-necked flask), the reaction mixture was stirred for an additional 5 min before it was passed through a 0.45  $\mu\text{m}$  PTFE syringe filter which was then washed with 2 mL of the reaction solvent (DCE or  $\text{CH}_2\text{Cl}_2$ ). Removal of the volatiles under reduced pressure afforded a solid residue that was dissolved in  $\text{CH}_2\text{Cl}_2$  and the filtration procedure was repeated. Thereafter, the product was dried under high vacuum (0.1 torr) for at least 6 h and then it was stored in a glovebox.

### 2.3.1 | Pyridinium tetrakis(3,5-bis (trifluoromethyl)phenyl)borate (PyrH)<sup>[30]</sup>

Pyridine (18.0  $\mu\text{L}$ , 17.7 mg, 0.223 mmol) and sodium tetrakis(3,5-bis (trifluoromethyl)phenyl)borate (202 mg, 0.228 mmol) in 2 mL of  $\text{CH}_2\text{Cl}_2$  were used. Following the general procedure led to 200 mg (95%) of a white solid (mp 194 – 196°C).  $^1\text{H}$  NMR (500 MHz,  $\text{CD}_2\text{Cl}_2$ )  $\delta$  12.25 (bs, 1H), 8.69–8.64 (m, 3H),<sup>[31]</sup> 8.13 (t,  $J = 7.0$  Hz, 2H), 7.73 (s, 8H), 7.57 (s, 4H).  $^{13}\text{C}$  NMR (125 MHz,  $\text{CD}_2\text{Cl}_2$ )  $\delta$  162.3 (q,  $^1J_{\text{B-C}} = 49.9$  Hz), 149.9, 141.4, 135.4, 129.5 (qq,  $^3J_{\text{B-C}} = 3.0$  Hz and  $^2J_{\text{F-C}} = 31.2$  Hz), 129.4, 125.2 (q,  $^1J_{\text{F-C}} = 272$  Hz), 118.1 (sept,  $^3J_{\text{F-C}} = 4.0$  Hz).<sup>[26]</sup>  $^{19}\text{F}$  (376 MHz,  $\text{CD}_2\text{Cl}_2$ )  $\delta$  -62.6. IR (ATR source) 3379, 1609, 1541, 1354, 1274, 1115  $\text{cm}^{-1}$ .

### 2.3.2 | 3-Hydroxypyridinium tetrakis(3,5-bis (trifluoromethyl)phenyl) borate (3H)

3-Hydroxypyridine (15.1 mg, 0.159 mmol) and sodium tetrakis(3,5-bis (trifluoromethyl)phenyl)borate (141 mg, 0.159 mmol) in 1.5 mL of  $\text{CH}_2\text{Cl}_2$  were used. Following the general procedure led to 137 mg (91%) of an off-white solid (mp 178 – 180°C).  $^1\text{H}$  NMR (500 MHz,  $\text{CD}_2\text{Cl}_2$ )  $\delta$  11.61 (NH, tt,  $J_{\text{N-H}} = 65.0$  Hz and  $J = 7.2$  Hz, 1H), 8.29–8.27 (m, 2H), 8.14–8.12 (m, 1H), 8.00 (t,  $J = 7.4$  Hz, 1H), 7.73 (s, 8H), 7.56 (s, 4H), 6.48 (s, OH, 1H).  $^{13}\text{C}$  NMR (125 MHz,  $d_6$ -DMSO)  $\delta$  161.0 (q,  $^1J_{\text{B-C}} = 49.5$  Hz), 156.2, 134.1, 133.5, 131.5, 130.6, 128.5 (qq,  $^3J_{\text{B-C}} = 2.9$  Hz and  $^2J_{\text{F-C}} = 31.5$  Hz), 127.7, 124.0 (q,  $^1J_{\text{F-C}} = 273$  Hz), 117.7 (sept,  $^3J_{\text{F-C}} = 3.6$  Hz).<sup>[24]</sup>  $^{19}\text{F}$  (376 MHz,  $\text{CD}_2\text{Cl}_2$ )  $\delta$  -62.7. IR (ATR source) 3582, 3527, 3379, 1610, 1559, 1355, 1274, 1104  $\text{cm}^{-1}$ . HRMS-ESI: calcd for  $\text{C}_5\text{H}_6\text{NO}$  ( $\text{M} - \text{C}_{32}\text{H}_{12}\text{BF}_{24}^-$ )<sup>+</sup> 96.0449, found 96.0436.

### 2.3.3 | 2-Hydroxypyridinium tetrakis(3,5-bis (trifluoromethyl)phenyl) borate (2H)

2-Hydroxypyridine (11.9 mg, 0.125 mmol) and sodium tetrakis(3,5-bis (trifluoromethyl)phenyl)borate (112 mg, 0.126 mmol) in 1.5 mL of  $\text{CH}_2\text{Cl}_2$  were used. Following the general procedure led to 91.4 mg (76%) of a white powder (mp 113 – 115°C).  $^1\text{H}$  NMR (500 MHz,  $\text{CD}_2\text{Cl}_2$ )  $\delta$  10.77 (NH, t,  $J_{\text{N-H}} = 60$  Hz, 1H), 8.86 (bs, OH, 1H), 8.40 (t,  $J = 7.8$  Hz, 1H), 8.09 (bs, 1H), 7.73 (s, 8H), 7.56 (s, 4H), 7.50 (t,  $J = 7.0$  Hz, 1H), 7.37 (d,  $J = 7.4$  Hz, 1H).  $^{13}\text{C}$  NMR (125 MHz,  $\text{CD}_2\text{Cl}_2$ )  $\delta$  162.3

(q,  $^1J_{B-C} = 49.9$  Hz), 161.9, 151.4, 137.4, 135.3, 129.5 (qq,  $^3J_{B-C} = 3.0$  Hz and  $^2J_{F-C} = 31.4$  Hz), 125.1 (q,  $^1J_{F-C} = 273$  Hz), 120.2, 118.1 (sept,  $^3J_{F-C} = 4.0$  Hz),<sup>[26]</sup> 115.4.  $^{19}\text{F}$  (376 MHz,  $\text{CD}_2\text{Cl}_2$ )  $\delta$  -62.7. IR (ATR source) 3542, 3369, 1649, 1633, 1610, 1543, 1354, 1273, 1112  $\text{cm}^{-1}$ . HRMS-ESI: calcd for  $\text{C}_5\text{H}_6\text{NO}$  ( $\text{M} - \text{C}_{32}\text{H}_{12}\text{BF}_{24}^-$ )<sup>+</sup> 96.0449, found 96.0440.

### 2.3.4 | N-Methyl-4-hydroxypyridinium tetrakis(3,5-bis (trifluoromethyl)phenyl) borate (4Me)

*N*-Methyl-4-pyridone (11.3 mg, 0.104 mmol) and sodium tetrakis(3,5-bis (trifluoromethyl)phenyl)-borate (93.3 mg, 0.105 mmol) in 2 mL of DCE were used. Following the general procedure led to 82.3 mg (82%) of a white powder (mp 148 – 150°C); residual DCE was removed by redissolving the material in 1 mL of  $\text{CH}_2\text{Cl}_2$  and removing the solvent with a rotary evaporator (20 torr), and then repeating this process at least 3 times.  $^1\text{H}$  NMR (500 MHz,  $\text{CD}_2\text{Cl}_2$ )  $\delta$  8.80 (OH, bs, 1H), 8.10 (d,  $J = 6.6$  Hz, 2H), 7.73 (s, 8H), 7.56 (s, 4H), 7.25 (d,  $J = 6.5$  Hz, 2H), 4.10 (s, 3H).  $^{13}\text{C}$  NMR (125 MHz,  $\text{CD}_2\text{Cl}_2$ )  $\delta$  170.5, 162.3 (q,  $^1J_{B-C} = 49.5$  Hz), 146.1, 135.3, 129.5 (qq,  $^3J_{B-C} = 3.2$  Hz and  $^2J_{F-C} = 31.6$  Hz), 125.1 (q,  $^1J_{F-C} = 273$  Hz), 118.1 (sept,  $^3J_{F-C} = 4.1$  Hz),<sup>[26]</sup> 116.4, 47.7.  $^{19}\text{F}$  (376 MHz,  $\text{CD}_2\text{Cl}_2$ )  $\delta$  -62.7. IR (ATR source) 3562, 3495, 1649, 1610, 1533, 1502, 1353, 1272, 1104  $\text{cm}^{-1}$ . HRMS-ESI: calcd for  $\text{C}_6\text{H}_8\text{NO}$  ( $\text{M} - \text{C}_{32}\text{H}_{12}\text{BF}_{24}^-$ )<sup>+</sup> 110.0606, found 110.0587.

### 2.3.5 | 2-Methoxypyridinium tetrakis(3,5-bis (trifluoromethyl)phenyl) borate (2MeOPyrH)

2-Methoxypyridine (12.5  $\mu\text{L}$ , 13.0 mg, 0.119 mmol) and sodium tetrakis(3,5-bis (trifluoromethyl)phenyl)borate (115 mg, 0.130 mmol) in 2.0 mL of  $\text{CH}_2\text{Cl}_2$  were used. Following the general procedure led to 112 mg (97%) of a white powder (mp 163 – 165°C).  $^1\text{H}$  NMR (500 MHz,  $\text{CD}_2\text{Cl}_2$ )  $\delta$  8.46 (ddd,  $J = 9.2$ , 7.4, and 1.8 Hz, 1H), 8.10 (dd,  $J = 6.2$  and 2.1 Hz, 1H), 7.73 (s, 8H), 7.56 (s, 4H), 7.49 (t,  $J = 6.8$  Hz, 1H), 7.35 (d,  $J = 9.0$  Hz, 1H), 4.21 (s, 3H), missing NH.  $^{13}\text{C}$  NMR (125 MHz,  $\text{CD}_2\text{Cl}_2$ )  $\delta$  162.3 (q,  $^1J_{B-C} = 50.0$  Hz), 161.2, 151.4, 138.4, 135.4, 129.5 (qq,  $^3J_{B-C} = 3.2$  Hz and  $^2J_{F-C} = 31.6$  Hz), 125.1 (q,  $^1J_{F-C} = 273$  Hz), 119.9, 118.1 (sept,  $^3J_{F-C} = 4.1$  Hz),<sup>[26]</sup> 111.3, 59.7.  $^{19}\text{F}$  (376 MHz,  $\text{CD}_2\text{Cl}_2$ )  $\delta$  -62.7. IR (ATR source) 3372, 1644, 16118, 1545, 1353, 1273, 1113  $\text{cm}^{-1}$ . HRMS-ESI: calcd for  $\text{C}_6\text{H}_8\text{NO}$  ( $\text{M} - \text{C}_{32}\text{H}_{12}\text{BF}_{24}^-$ )<sup>+</sup> 110.0606, found 110.0585.

## 2.4 | General procedure for dimerization determinations with $^1\text{H}$ NMR spectroscopy

A solution of known concentration consisting of **3Me**, **3H**, **4H**, and **2MeOPyrH** was made in  $\text{CD}_2\text{Cl}_2$  and an aliquot (0.5 mL) was transferred into a 9" NMR tube. An initial spectrum was obtained before additional  $\text{CD}_2\text{Cl}_2$  (0.1–0.5 mL) was added and mixed by inverting the NMR tube twice. Another spectrum was recorded and this process was repeated multiple times before carrying out a non-linear fit of the data using the BindFit program (see below) to obtain the corresponding dimerization constants.

## 2.5 | General kinetic study procedure for the Friedel-Crafts reaction of *N*-methylindole with *trans*- $\beta$ -nitrostyrene

In a 1 mL volumetric flask, 74.6 mg (0.500 mmol) of *trans*- $\beta$ -nitrostyrene, 6.2  $\mu\text{L}$  (6.5 mg, 0.050 mmol) of *N*-methylindole, and the catalyst (0.005 mmol) were added and dissolved in  $\text{CD}_2\text{Cl}_2$  to a total volume of 1 mL. The flask was stoppered, and inverted twice to ensure good mixing, and then the entire contents were transferred to an NMR tube which was capped and sealed with electrical tape. A  $^1\text{H}$  NMR spectrum was taken as soon as possible (within 10 minutes of mixing) and when the sample was not in the NMR spectrometer, it was submerged in a 27°C water bath. Reaction conversions were calculated using the signals at 6.47 and 5.20 – 4.96 ppm for *N*-methylindole and the product, respectively, and a pseudo-first-order kinetic model was employed.

## 2.6 | General procedure for UV titrations<sup>8, 10d</sup>

### 2.6.1 | Solution preparation

In a 1 mL volumetric flask, 1.0–1.5 mg of the sensor was dissolved in  $\text{CH}_2\text{Cl}_2$  to the line in the glassware. In a 5 mL volumetric flask, 25  $\mu\text{L}$  of the 1 mg/mL sensor solution was added and then was diluted to the line with  $\text{CH}_2\text{Cl}_2$  (solution A). In a separate 5 mL volumetric flask containing 20–30 equivalents of the Brønsted acid, another 25  $\mu\text{L}$  of the 1 mg/mL sensor solution was added and diluted to the line with  $\text{CH}_2\text{Cl}_2$  (solution B).

### 2.6.2 | Titration procedure

In a 10 mm cuvette with a screwcap top, 2 mL of solution A was added and the vessel was sealed with a

PTFE septum. After collecting the background of only  $\text{CH}_2\text{Cl}_2$ , a spectrum of the free sensor from 300 to 950 nm was obtained and the  $\lambda_{\text{max}}$  and the absorbance value at  $\lambda_{\text{max}}$  were recorded. Then an aliquot (10–15  $\mu\text{L}$ ) of solution B was added by microsyringe to the cuvette which was then shaken for 15–20 seconds, and then another spectrum was collected. The new  $\lambda_{\text{max}}$  and its corresponding absorbance value were recorded and cuvette was shaken again (15–20 seconds) and the spectrum was recollected to ensure that  $\lambda_{\text{max}}$  and the absorbance at  $\lambda_{\text{max}}$  were invariant. If significant changes were observed (greater than  $\pm 1$  for  $\lambda_{\text{max}}$  or  $\pm 0.010$  for the absorbance), the mixture was shaken again and another spectrum was collected until the data was consistent (in general, no more than 4 repetitions were needed). Then another portion (10–15  $\mu\text{L}$ ) of solution B was added and the collection procedure was repeated. As the titration went along, the amount of titrant (solution B) could be increased (20 – 500  $\mu\text{L}$ ) until the observed  $\lambda_{\text{max}}$  and the absorbance value did not change after 2 consecutive additions.

### 2.6.3 | Calculating the binding constants

Absorbance values from 4 different wavelengths and the equivalents of Brønsted acid to sensor were used to calculate the binding constant ( $K$ ). The  $\lambda_{\text{max}}$  of the free sensor (~500 nm) and of the bound complex, and wavelengths 30 nm above (~530 nm) and below those values were used in the analysis. These data points were nonlinearly fit with the BindFit app (<http://app.supramolecular.org/bindfit/>) for 1:1, 1:2, and 2:1 sensor to catalyst relationships to obtain the binding constants and the statistical errors.

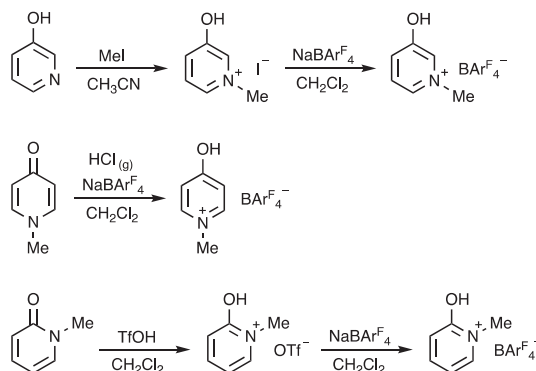
### 2.7 | Computations

DFT (B3LYP/6-31G(2df,p), B3LYP/cc-pVDZ, B3LYP/cc-pVTZ//B3LYP/cc-pVDZ, M06-2X/cc-pVDZ and M06-2X/cc-pVTZ//M06-2X/p-VTZ)<sup>[32,33]</sup> and G4-theory<sup>[19]</sup> computations were carried out using Gaussian 16 at the Minnesota Supercomputer Institute for Computational Chemistry or on a desktop MacIntosh computer with GaussView 6.<sup>[34,35]</sup> All structures were fully optimized and correspond to minima on the potential energy surface (i.e., all of the vibrational frequencies correspond to positive values). Geometries, energies and select vibrational frequencies are provided in the Supporting Information.

## 3 | RESULTS AND DISCUSSION

### 3.1 | Model catalysts syntheses

*N*-Methyl-3-hydroxypyridinium  $\text{BARF}_4$  (**3Me**) was prepared by reacting 3-hydroxypyridine with methyl iodide to afford *N*-methyl-3-hydroxypyridinium iodide, which was then converted to the  $\text{BARF}_4$  salt by anion exchange with  $\text{NaBARF}_4$  in dichloromethane (Scheme 2).<sup>[36]</sup> Alkylation of 2- and 4-hydroxypyridine in a similar manner afforded a mixture of *N*- and *O*-alkylated products due to the tautomeric nature of the starting substrates,<sup>[37,38]</sup> and we were unable to obtain dry samples of the separated species. Protonation of the corresponding *N*-methylpyridones, consequently was explored. Aqueous acids (HI and HCl) led to the desired halide salts but problems were encountered in trying to remove water from these compounds. To circumvent this issue, a one pot protonation and anion exchange procedure was developed. Anhydrous HCl gas was produced *in situ*<sup>[29]</sup> and bubbled through a dichloromethane or 1,2-dichloroethane solution containing the pyridone of interest and  $\text{NaBARF}_4$ . This successfully led to **4Me** but a minor byproduct that resisted purification arose in the preparation of **2Me**; we speculate that this impurity is an isomer of **2Me** and corresponds to *N*-protonation of *N*-methyl-2-pyridone. A satisfactory sample of the latter compound was generated via its triflate salt, which is easier to handle and purify than the corresponding halides, by reacting *N*-methyl-2-pyridone with neat triflic acid and taking advantage of the differential solubility of  $\text{NaOTf}$  and  $\text{NaBARF}_4$  in dichloromethane. The one pot procedure with gaseous HCl was also used to synthesize protonated pyridinium salts **2H**, **3H**, and **PyrH**, but not **4H** since 4-hydroxypyridine is insufficiently soluble in  $\text{CH}_2\text{Cl}_2$ . In this latter case, **4H** was prepared from its triflate salt in an analogous manner to **2Me**.



**SCHEME 2** Synthetic routes for all three isomeric *N*-methylhydroxypyridinium  $\text{BARF}_4$  salts



### 3.2 | IR studies

IR spectroscopy was used to assess the acidities and hydrogen bond donating abilities of the *N*-methylated phenols in a nonpolar solvent. These salts are insufficiently soluble in carbon tetrachloride, the solvent that was previously utilized,<sup>[9]</sup> so dichloromethane-*d*<sub>2</sub> was used instead. The free and hydrogen bound O–H stretching frequencies for **2Me**, **3Me**, **4Me**, phenol, and 4-nitrophenol were obtained in CD<sub>2</sub>Cl<sub>2</sub> and a 1% (v/v) mixture of CD<sub>3</sub>CN in CD<sub>2</sub>Cl<sub>2</sub> (Table 1). Gas-phase acidities ( $\Delta G^\circ_{\text{acid}}$ ) of these compounds were computed at 298 K using the highly accurate G4 composite approach and are also given in Table 1.

As shown in entries 1–5 in Table 1, a larger  $\Delta\nu$  was observed for more acidic compounds with smaller  $\Delta G^\circ_{\text{acid}}$  values. For example, phenol has a gas-phase acidity of 341.5 kcal mol<sup>−1</sup> and afforded a difference in the O–H stretch of 170 cm<sup>−1</sup> (entry 1), whereas  $\Delta G^\circ_{\text{acid}} = 227.0$  kcal mol<sup>−1</sup> for **4Me** and a frequency change of 398 cm<sup>−1</sup> (entry 4) was found. The same trend was observed with the free O–H stretches with the possible exception of **2Me**, but the range was approximately four times smaller (i.e., 435 vs 102 cm<sup>−1</sup> or ~4 vs 1 mol cm<sup>−1</sup> kcal<sup>−1</sup> given that the acidities span 114.5 kcal mol<sup>−1</sup> from 341.5 to 227.0 kcal mol<sup>−1</sup>).<sup>[40]</sup>

Two acidic sites are present in the protonated series of hydroxypyridines, and as expected, the O–H acidities for **2H**–**4H** follow the same trend as **2Me**–**4Me** (i.e., **2Me** (most acidic) > **4Me** > **3Me** (least acidic)). The N–H

positions are calculated to be the more acidic sites, but the differences are small for **2H** and **4H** (i.e., 0.9 and 3.5 kcal mol<sup>−1</sup>, respectively) due to tautomer formation upon O-deprotonation in these cases. In contrast, a zwitterion results from **3H** and the G4 acidity difference is much larger (i.e., 15.1 kcal mol<sup>−1</sup>). A different acidity ordering of **2H** > **3H** > **4H** is found, and is surprising since one would expect the relative stabilities of these ions (i.e., **4H** (0) > **2H** (0.5) > **3H** (6.0 kcal mol<sup>−1</sup>)) to be inversely related to their acidities. 2-Hydroxypyridine is 9.5 kcal mol<sup>−1</sup> more stable than 3-hydroxypyridine, however, due to a favorable O–H...N electrostatic interaction. This energy difference is larger than that between **2H** and **3H**, and is sufficient to reverse their acidities and account for why **2H** is the more acidic compound.

Both the N–H and O–H stretching frequencies for **2H**–**4H** in the presence and absence of CD<sub>3</sub>CN are given in Table 1. Computed values for all of the acids listed in entries 1–9 along with their acetonitrile complexes are provided in the Supporting Information, and the former and latter values are linearly correlated with the observed stretching frequencies (Figures S2 and S3, respectively). As expected,  $\Delta\nu$  for both the N–H and O–H stretches correlate with the gas-phase acidities of these positions although the linear correlation is much tighter for the more acidic site (Figure 2).

This is not surprising since one would expect the initial acetonitrile to bind at the more acidic N–H position and only subsequently coordinate at the O–H site.

**TABLE 1** IR O–H and N–H stretching frequencies and gas-phase acidities of a series of phenol and pyridinium derivatives<sup>a</sup>

Entry	Cmpd	$\nu$ (cm <sup>−1</sup> ) <sup>b</sup>		$\Delta\nu$ (cm <sup>−1</sup> ) <sup>b, c</sup>	$\Delta G^\circ_{\text{acid}}$ (kcal mol <sup>−1</sup> ) <sup>b, d</sup>
		CD <sub>2</sub> Cl <sub>2</sub>	1% CD <sub>3</sub> CN		
1	C <sub>6</sub> H <sub>5</sub> OH	3582	3412	170 [157]	341.7
2	4-O <sub>2</sub> NC <sub>6</sub> H <sub>4</sub> OH	3559	3330	229 [221]	320.6
3	<b>2Me</b>	<3501> <sup>e</sup>	2977	524	215.5
4	<b>3Me</b>	3513	3179	334 [370] <sup>f</sup>	234.3
5	<b>4Me</b>	3480	3082	398	227.0
6	<b>PyrH</b>	(3307)	(2903)	(306)	(214.9) <sup>h</sup>
7	<b>2H</b> <sup>g</sup>	<3499> <sup>e</sup> (3316)	3071 (2962)	428 (354)	211.9 (211.0)
8	<b>3H</b> <sup>g</sup>	3516 (3308)	3193 (2902)	323 (300)	230.1 (215.0)
9	<b>4H</b> <sup>g</sup>	3477 (3348)	3249 (3107)	228 (241)	222.2 (218.7)

<sup>a</sup>Spectra collected using ~5 mM solutions of each compound in a 1 mm liquid cell.

<sup>b</sup>Parenthetical numbers are for N–H stretches or acidities.

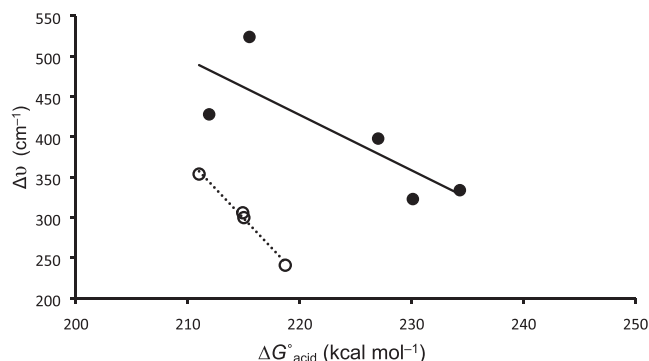
<sup>c</sup>Values in brackets were obtained in CCl<sub>4</sub> and taken from ref. [9].

<sup>d</sup>Computed G4 theory values. Experimental acidities of 341.5 (PhOH), 320.9 (4-O<sub>2</sub>NC<sub>6</sub>H<sub>4</sub>OH), 213.9 (**2Me**), 214.9 (**PyrH**), and 214.6 (**3H**) kcal mol<sup>−1</sup> have been reported; see ref. [39].

<sup>e</sup>The O–H stretch was not observed and the given value is a scaled (0.923) B3LYP/6-31G(2df,p) vibrational frequency.

<sup>f</sup>This value is for *N*-octyl-3-hydroxypyridinium BAr<sup>F</sup><sub>4</sub>.

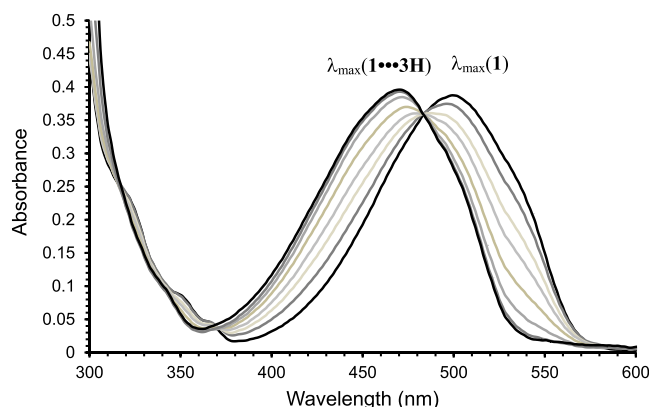
<sup>g</sup>Free energies for the hydroxypyridines are computed to be lower in energy than the corresponding pyridones (a zwitterion in the case of **3H**) by 0.93 (**2H**), 3.46 (**4H**), and 15.1 (**3H**) kcal mol<sup>−1</sup>.



**FIGURE 2** Changes in the N-H (open circles) and O-H (filled circles) IR frequencies of pyridinium  $\text{BARF}_4^-$  salts in  $\text{CD}_2\text{Cl}_2$  upon addition of  $\text{CD}_3\text{CN}$  versus the corresponding gas-phase G4 acidities of the free ions. Linear least squares fits provide the following equations:  $\Delta\nu (\text{cm}^{-1}) = -14.7 \times \Delta G^\circ_{\text{acid}} + 3451$ ,  $r^2 = 0.991$  (N-H acids) and  $\Delta\nu (\text{cm}^{-1}) = -6.87 \times \Delta G^\circ_{\text{acid}} + 1939$ ,  $r^2 = 0.662$  (O-H acids with **4H** omitted and not shown)

### 3.3 | UV-Vis studies

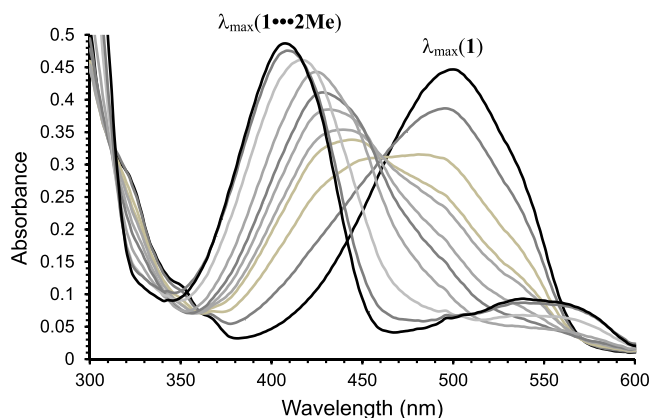
An alternative approach for assessing acids in non-polar solvents is to titrate them with a colorimetric hydrogen bond accepting sensor (**1**), and monitor the resulting UV-vis spectra to obtain changes in the absorption maxima along with 1:1 association binding constants.<sup>8, 10d</sup> An updated procedure was developed involving a non-linear fit of the binding isotherm data, and well-defined isosbestic points were observed with **3Me**, **4Me**, **3H**, and **PyrH**. For example, over the course of adding 10 equivalents of **3H** to **1** (Figure 3) an isosbestic point at 484 nm is observed and  $\lambda_{\text{max}}$  of the bound complex at 471 nm is readily obtained. These observations are consistent with a single intermediate being formed between the Brønsted acid and UV/vis sensor (i.e., 1:1 binding). Different



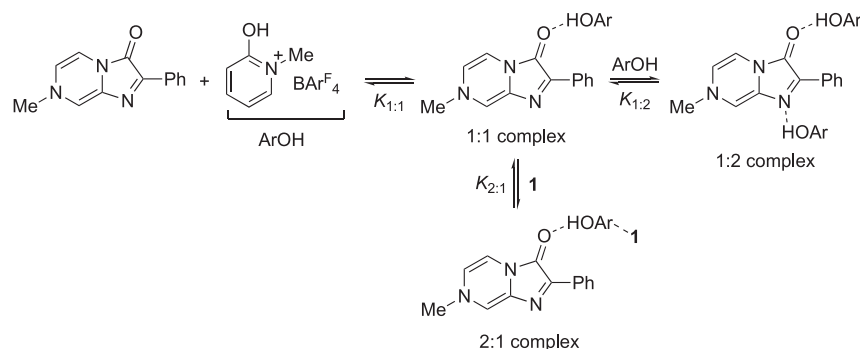
**FIGURE 3** UV-vis spectra from 300 to 600 nm for the titration of **1** with **3H**. For clarity only half of the spectra are shown and they correspond to the addition of 0.00, 0.35, 0.69, 1.02, 1.67, 2.89, 5.59, and 10.7 equivalents of **3H**

behavior was found for **2Me**, **2H**, and **4H** in that an apparent isosbestic point is seen only when up to about 1 equivalent of the phenol is added (Figure 4 and Figures S14 and S16).<sup>[41]</sup> It disappears upon further addition of the substrate due to a continuous blue shift that occurs throughout the titration. This makes it difficult to obtain  $\lambda_{\text{max}}$  for the 1:1 complex as there is no clear endpoint in the titration. A new band also grows in at higher concentrations of the hydrogen bond donor (e.g., the feature between 450 and 600 nm in Figure 4), and this led to different colored solutions for **2Me** and **2H**.<sup>[42]</sup> Taken together, these observations indicate that more than one species is formed in these three cases, and two or more equilibria are involved.

To account for all of the above results, 1:1, 1:2, and 2:1 interactions with **1** were considered for each of the pyridinium salts (Scheme 3). In the 1:2 complex, the two acids presumably interact with the carbonyl oxygen and the  $\beta$ -nitrogen atom. B3LYP/cc-pVTZ//B3LYP/cc-pVDZ and M06-2X/cc-pVTZ//M06-2X/cc-pVDZ computations on **1**•••PhOH are in accord with this view in that coordination at both of these sites are similar in energy. That is, the enthalpy at 298 K for binding at the carbonyl oxygen as opposed to the  $\beta$ -nitrogen is predicted to be favored by 2.11 and 1.37 kcal mol<sup>-1</sup>, respectively. Alternatively, two molecules of **1** can interact with a single substrate (i.e., 2:1 binding) if multiple hydrogen bonding sites are present in the catalyst, such as the N-H and O-H bonds in **2H**. For **2Me**, we speculated that the hydroxyl group and carbon-hydrogen bonds of the methyl substituent can serve as hydrogen bond donors.<sup>[43]</sup> To assess this possibility, *N*-methylpyridinium  $\text{BARF}_4^-$  (**PyrMe**) was prepared and examined. Its spectra were well behaved and a clean isosbestic point was observed indicating a 1:1 association with **1**. This strongly suggests that the carbon-



**FIGURE 4** UV-vis spectra from 300 to 600 nm for the titration of **2Me** with **1**. For clarity only half of the spectra are shown and they correspond to the addition of 0.00, 0.22, 0.44, 0.65, 0.76, 1.00, 1.50, 2.50, 5.80, 11.0, and 22.0 equivalents of **2Me**

**SCHEME 3** Proposed binding modes for Brønsted acids such as **2Me** with **1**

hydrogen bonds are sufficiently polarized to lead to a binding interaction. Equilibrium association constants were determined using the free online BindFit program and are given in Table 2.<sup>[44,45]</sup> As expected, those compounds that displayed clean isosbestic points throughout the titration are well fit by a 1:1 association model. The remaining three salts are best fit by 2:1 (**2Me** and **2H**) and 1:2 (**4H**) binding schemes, although the latter scenario can be viewed as a 1:1 interaction of **1** with the dimer of **4H**. To explore this possibility, <sup>1</sup>H NMR spectra of **4H** were recorded and the OH, NH, and aryl hydrogen chemical shifts were found to move downfield with increasing concentration. A nonlinear fit of these results afforded a monomer-dimer equilibrium constant ( $K_D$ ) of  $1.3 \times 10^3 \text{ M}^{-1}$ . Given this value, >99.99% of **4H** exists as a monomer at the mid-concentration used in the UV-vis titration with **1**. In contrast, **3H** and **3Me** (which afforded simple 1:1 behavior) were found to have smaller

dimerization equilibrium constants of  $3.3 \times 10^2$  and  $1.2 \times 10^2 \text{ M}^{-1}$ , respectively.<sup>[46]</sup> For both the methylated and protonated series of pyridinium ions the binding equilibrium constants follow the same order: **2** > **4** > **3** and  $\ln K$  is found to linearly correlate with  $\Delta G^\circ_{\text{acid}}$  for the six compounds that were fit by 1:1 or 1:2 binding models (Figure 5). The two ortho species (**2H** and **2Me**) are best described by 2:1 associations and their  $K_{1:1}$  values are smaller than expected given their computed acidities.

### 3.4 | Kinetics

Rate constants and reaction half-lives for the Friedel-Crafts alkylation of *N*-methylindole with *trans*- $\beta$ -nitrostyrene were obtained under pseudo-first order conditions (Table 3).<sup>[47]</sup> In the absence of a catalyst (entry 1), this transformation takes place extremely slowly and has an estimated half-life of 3700 h or 155 days. Upon

**TABLE 2** Wavelength shifts and binding constants from UV-vis titrations with **1**

Entry	Catalyst	Binding model	$\lambda_{\text{max}}^{1:1} \text{ (nm)}^{a,b}$	$K_{1:1} \text{ (M}^{-1}\text{)}^b$
1	<b>2Me</b> <sup>c</sup>	2:1	410.7	$3.47 \times 10^4$
2	<b>3Me</b>	1:1	472.1 (471.7)	$2.01 \times 10^4$
3	<b>4Me</b>	1:1	466.5 (465.6)	$1.23 \times 10^5$
4	<b>PyrMe</b>	1:1	474.9 (474.9)	$6.50 \times 10^2$
5	<b>PyrH</b>	1:1	470.3 (469.3)	$1.78 \times 10^5$
6	<b>2H</b> <sup>d</sup>	2:1	408.9	$4.71 \times 10^4$
7	<b>3H</b>	1:1	470.6 (470.3)	$6.05 \times 10^4$
8	<b>4H</b> <sup>e</sup>	1:2	463.5	$8.51 \times 10^4$

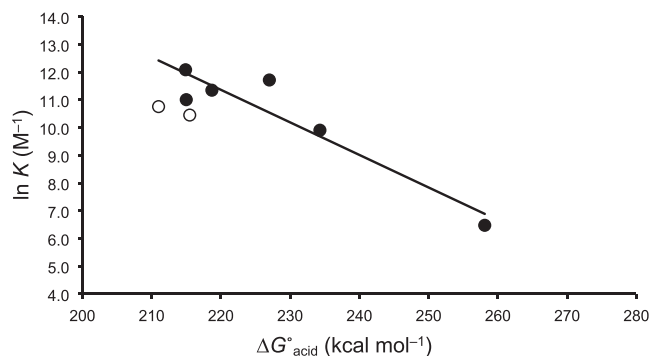
<sup>a</sup>Wavelengths for the absorption maxima of the 1:1 complexes were obtained from a plot of  $\chi/\lambda_{\text{max}}$  at each titration point, where  $\chi$  is the 1:1 mole fraction resulting from the fit of the data; for additional details, see the Supporting Information. Parenthetical values correspond to observed  $\lambda_{\text{max}}$  endpoints.

<sup>b</sup>Averages of duplicate measurements.

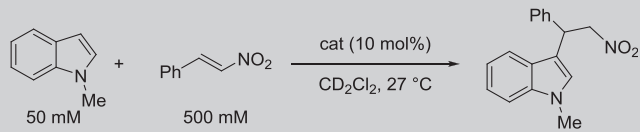
<sup>c</sup> $K_{2:1} = 1.44 \times 10^4 \text{ M}^{-1}$ .

<sup>d</sup> $K_{2:1} = 8.42 \times 10^3 \text{ M}^{-1}$ .

<sup>e</sup> $K_{1:2} = 1.23 \times 10^4 \text{ M}^{-1}$ .

**FIGURE 5** Linear least squares fit of the logarithms of the 1:1 equilibrium association constants between **1** and the pyridinium salts listed in Table 2 versus the G4 acidities of the pyridinium ions. The equation for the line is  $\ln K = -0.118 \times \Delta G^\circ_{\text{acid}} + 37.2$ ,  $r^2 = 0.882$ , and the values for **2H** and **2Me** (open circles) were omitted from the regression

**TABLE 3** Kinetic data for a Friedel-Crafts reaction between *N*-Methylindole and *trans*- $\beta$ -Nitrostyrene

				
Entry	Catalyst	$t_{1/2}$ (h) <sup>a</sup>	$k$ (h <sup>-1</sup> ) <sup>a</sup>	$k_{rel}$
1	-	3700	$1.86 \times 10^{-4}$	0.0022
2	 (2Me)	2.5	$2.73 \times 10^{-1}$	3.3
3	 (3Me)	8.3	$8.33 \times 10^{-2}$	1.0
4	 (4Me)	4.2	$1.67 \times 10^{-1}$	2.0
5	 (PyrMe) <sup>b</sup>	790	$8.89 \times 10^{-4}$	0.011
6	 (PyrH)	2.7	$2.58 \times 10^{-1}$	3.2

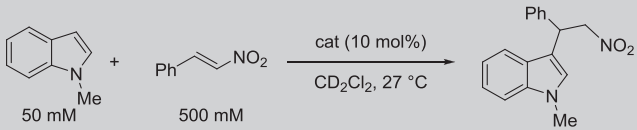
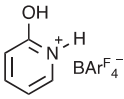
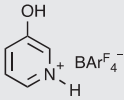
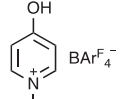
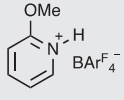
(Continues)

employing 10 mol% of **2Me–4Me** (entries 2–4), rate constants spanning from 0.083 to 0.27 h<sup>-1</sup> with half-lives between 2.5 and 8.3 h were observed. This leads to a reactivity order of **2Me** > **4Me** > **3Me**, which is in accord

with the IR data, the G4 acidities, and the UV-vis  $\lambda_{max}$  values for the 1:1 complexes noted above. The magnitudes of the 1:1 equilibrium binding constants for **2Me** and **4Me**, however, are reversed. To verify that **2Me**–



TABLE 3 (Continued)

				
Entry	Catalyst	$t_{1/2}$ (h) <sup>a</sup>	$k$ (h <sup>-1</sup> ) <sup>a</sup>	$k_{rel}$
7 <sup>c</sup>	 (2H)	0.47	1.49	18
8	 (3H)	2.9	$2.38 \times 10^{-1}$	2.9
9	 (4H)	3.7	$1.83 \times 10^{-1}$	2.2
10	 (2MeOPyrH)	5.9	$1.17 \times 10^{-1}$	1.4

<sup>a</sup>Average of duplicate trials.<sup>b</sup>Background corrected data.<sup>c</sup>T = 25 °C.

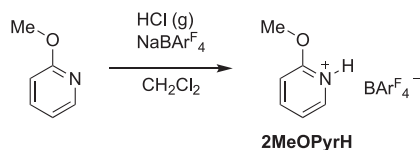
**4Me** are functioning as O–H hydrogen bond donating catalysts, **PyrMe** was also examined (entry 5) since the UV-vis data revealed that it associates with **1** even though the hydroxyl group is absent. This species does catalyze the Friedel-Crafts reaction relative to the background process even though all of the hydrogens are attached to carbon atoms, but it is ~100–300 times less effective than **2Me–4Me**. This is in accord with the UV-vis results (i.e.,  $\lambda_{max}$  and  $K$ ) and is consistent with the *N*-

methylhydroxypyridinium ions serving as O–H hydrogen bond donors.

For the protonated series of hydroxypyridinium  $\text{BAr}^{\text{F}_4-}$  salts (entries 6–9), the reactivity order is **2H** > **PyrH**, **3-H** > **4H** and the half-lives range from under 30 minutes to 4 hours. Both **PyrH** and **3H** have similar catalytic activities, and this suggests that the latter species also acts as a N–H hydrogen bond donor rather than an O–H Brønsted acid. The same conclusion can be

drawn for **2H** and **4H** since the the protonated catalysts lead to faster reactions than their corresponding *N*-methylated analogues (i.e., **2H** > **2Me**, **3H** > **3Me** and **4H** > **4Me**). Interestingly, **2H** is significantly more active than all of the other catalysts (entry 7), which implies that bidentate activation involving both the N–H and O–H sites occurs in this case. To assess this possibility, 2-methoxypyridinium  $\text{BAR}^{\text{F}_4}$  (**2MeOPyrH**) was prepared from 2-methoxypyridine (Scheme 4)<sup>[48]</sup> following the one pot protonation and anion exchange method described above. This compound is electronically similar to **2H** and **4H**, but is missing the O–H hydrogen bond donating site. Its catalytic ability (entry 10) is comparable to **4H** (half-lives of ~6 and 4 h, respectively), but is more than an order of magnitude less than that for **2H**. Given that the dimerization equilibrium constant determined by <sup>1</sup>H NMR for **2MeOPyrH** is only 22  $\text{M}^{-1}$  and a factor of 10–100 times smaller than for **3H**, **3Me**, and **4H**,<sup>[49]</sup> it is likely that **2H** employs both N–H and O–H hydrogen bonds to activate *trans*- $\beta$ -nitrostyrene for nucleophilic attack by *N*-methylindole.

In an analogous fashion to the *N*-methylated pyridinium ions, the reaction rate data for the *N*-protonated catalysts correlate with the IR vibrational frequency changes ( $\Delta\nu$ ) in the N–H and O–H stretching



**SCHEME 4** Synthesis of control compound **2MeOPyrH**

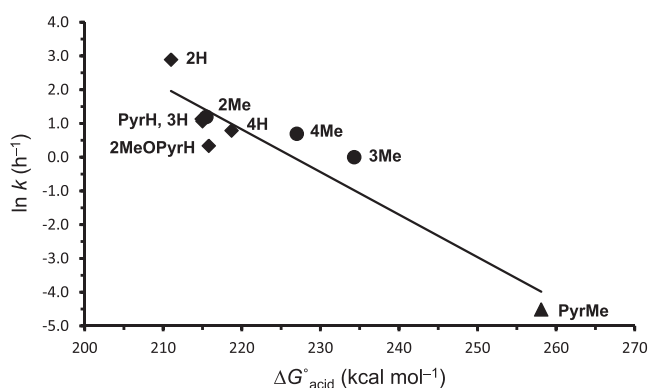


**FIGURE 6** Logarithm of experimental rate constants vs computed G4 gas-phase acidities. A linear least squares fit using all 9 catalysts in Table 3 gives  $\ln k = -0.126 \times \Delta G^\circ_{\text{acid}} + 28.6$ ,  $r^2 = 0.875$  whereas omission of **2MeOPyrH** leads to  $\ln k = -0.131 \times \Delta G^\circ_{\text{acid}} + 29.9$ ,  $r^2 = 0.912$  (not shown). Circles, diamonds, and triangles are used for **2Me–4Me** (O–H acids), **2H–4H**, **PyrH**, and **2MeOPyrH** (N–H acids), and **PyrMe** (C–H acids), respectively

modes. Neither  $\lambda_{\text{max}}$  or the 1:1 equilibrium binding constants from the UV-vis titration experiments with **1**, however, are good measures of the catalyst activities. This break-down in the latter approach presumably is related to the higher-order binding obtained with **2H** and **4H**. A plot of the logarithm of the experimental reaction rate constants versus the computed G4 gas-phase acidities of the pyridinium ions provides a reasonable linear correlation for all nine catalysts listed in Table 3 (Figure 6) even though these compounds include N–H, O–H, and C–H hydrogen bond donors and the counteranion is not accounted for in the calculations.

## 4 | CONCLUSIONS

All three isomers of both the *N*-methylated and *N*-protonated hydroxypyridinium  $\text{BAR}^{\text{F}_4}$  salts along with several reference compounds were investigated. DFT and G4 theory computations, IR, UV-vis, and kinetic studies revealed the effects of changing the relative position of the charged center to the ionization site, and the consequences of having one (O–H) or two (O–H and N–H) hydrogen bond donating groups. Calculated gas-phase acidities of the corresponding cations without their  $\text{BAR}^{\text{F}_4}$  counteranion were found to be good predictors of the hydrogen bond donating abilities of these salts, and are linearly correlated with IR and UV-vis spectroscopic results and pseudo-first-order rate constants. As a result, changes in the IR stretching frequencies of the O–H and N–H bonds in the absence and presence of a hydrogen bond acceptor ( $\Delta\nu$ ) are reliable indicators of their relative reactivity orders (i.e., O–H acids and separately N–H acids). In a similar manner, 1:1 equilibrium association constants obtained by UV-vis monitored titrations with a colorimetric sensor (**1**) are good measures of the catalytic abilities of O–H (**3Me**, **4Me**), N–H (**PyrH**, **3H**, **4H**) and C–H (**PyrMe**) Brønsted acids. This correlation breaks down, however, for **2Me** and **2H**, both of which failed to give an isosbestic point and were found to associate with two molecules of **1** (i.e., 2:1 binding).

Alkyl pyridinium ions with the charge center meta to the ionization site have been the most widely employed charge-enhanced structures to come from our laboratory. These species avoid introducing an additional O–H or N–H hydrogen bond donating site or resonance delocalization effects. The latter interactions as reflected by comparisons of **2Me** and **4Me** relative to **3Me** were found to lead to catalysts that are several times more reactive in the Friedel-Crafts alkylation of *N*-methylindole with *trans*- $\beta$ -nitrostyrene. Introduction of the charged-center by protonation leads to more acidic compounds, alters the interaction site with the substrate, and affords

modestly more active catalysts. The one exception is **2H**, which due to the ortho arrangement of its two acidic sites presumably leads to bidentate activation, and resulted in a significantly larger rate enhancement. This type of structural modification can lead to more rigid complexes and transition state structures providing a means for more closely mimicking enzymes and designing more reactive charge-activated catalysts.

## NOTES

The authors declare no competing financial interest.

## ACKNOWLEDGEMENTS

We would like to thank Ms. Grace Gast for her preliminary investigations on this project, Mr. Serdar Yalvac for his contributions toward developing the UV-vis titration procedure, and Prof. Phillipe Buhlmann for helpful discussions and his guidance regarding titrations that result in multiple binding equilibria. Generous support from the National Science Foundation (CHE-1665392) and the Minnesota Supercomputer Institute for Advanced Computational Research are also gratefully acknowledged.

## ORCID

Curtis Payne  <https://orcid.org/0000-0001-9100-2375>

Steven R. Kass  <https://orcid.org/0000-0001-7007-9322>

## REFERENCES

- [1] a) K. B. Schowen, H.-H. Limbach, G. S. Denisov, R. L. Schowen, *Biochim. Biophys. Acta* **2000**, 1458, 43. b) L. Simon, J. M. Goodman, *J. Org. Chem.* **2010**, 75, 1831. c) D. Röthlisberger, O. Khersonsky, A. M. Wollacott, L. Jiang, J. DeChancie, J. Betker, J. L. Gallaher, E. A. Althoff, A. Zanghellini, O. Dym, S. Albeck, K. N. Houk, D. S. Tawfik, D. Baker, *Nature* **2008**, 453, 190.
- [2] R. R. Knowles, E. N. Jacobsen, *Proc. Natl. Acad. Sci. U. S. A.* **2010**, 107, 20678.
- [3] a) A. G. Doyle, E. N. Jacobsen, *Chem. Rev.* **2007**, 107, 5713. b) F. Giacalone, M. Gruttadauria, P. Agrigento, R. Noto, *Chem. Soc. Rev.* **2012**, 41, 2406. c) R. C. Wende, P. R. Schreiner, *Green Chem.* **2012**, 14, 1821. d) R. J. Phipps, G. L. Hamilton, F. D. Toste, *Nat. Chem.* **2012**, 4, 603.
- [4] a) J. Hine, S.-M. Linden, V. M. Kanagasabapathy, *J. Am. Chem. Soc.* **1985**, 107, 1082. b) K. H. Jensen, M. S. Sigman, *J. Org. Chem.* **2010**, 75, 7194. c) K. Kaupmees, N. Tolstoluzhsky, S. Raja, M. Rueping, I. Leito, *Angew. Chem. Int. Ed.* **2013**, 52, 11569.
- [5] a) T. J. Auvi, A. G. Schafer, A. E. Mattson, *Eur. J. Org. Chem.* **2014**, 2014, 2633. b) T. Akiyama, *Chem. Rev.* **2007**, 107, 5744. c) T. Akiyama, K. Mori, *Chem. Rev.* **2015**, 115, 9277.
- [6] a) P. R. Schreiner, A. Wittkopp, *Org. Lett.* **2002**, 4, 217. b) A. Wittkopp, P. R. Schreiner, *Chem. A Eur. J.* **2003**, 9, 407. c) K. M. Lippert, K. Hof, D. Gerbig, D. Ley, H. Hausmann, S. Guenther, P. R. Schreiner, *Eur. J. Org. Chem.* **2012**, 2012, 5919. d) Z. Zhang, Z. Bao, H. Xing, *Org. Biomol. Chem.* **2014**, 12, 3151.
- [7] a) F. G. Bordwell, *Acc. Chem. Res.* **1988**, 21, 456. b) S. Tshepelevitsh, A. Kütt, M. Lökov, I. Kaijurand, J. Saame, A. Heering, P. G. Plieger, R. Vianello, I. Leito, *Eur. J. Org. Chem.* **2019**, 2019, 6735. c) M. Lökov, S. Tshepelevitsh, A. Heering, P. G. Plieger, R. Vianello, I. Leito, *Eur. J. Org. Chem.* **2017**, 2017, 4475.
- [8] a) P. N. H. Huynh, R. R. Walvoord, M. C. Kozlowski, *J. Am. Chem. Soc.* **2012**, 134, 15621. b) R. R. Walvoord, P. N. H. Huynh, M. C. Kozlowski, *J. Am. Chem. Soc.* **2014**, 136, 16055.
- [9] M. Samet, J. Buhle, Y. Zhou, S. R. Kass, *J. Am. Chem. Soc.* **2015**, 137, 4678.
- [10] a) Y. Fan, S. R. Kass, *Org. Lett.* **2016**, 18, 188. b) Y. Fan, S. R. Kass, *J. Org. Chem.* **2017**, 82, 13288. c) Y. Fan, M. Tiffner, J. Schorgerhumer, R. Robiette, M. Waser, S. R. Kass, *J. Org. Chem.* **2018**, 83, 9991. d) Y. Fan, C. Payne, S. R. Kass, *J. Org. Chem.* **2018**, 83, 10855.
- [11] a) J. Ma, S. R. Kass, *Org. Lett.* **2016**, 18, 5812. b) J. Ma, S. R. Kass, *Org. Lett.* **2018**, 20, 2689. c) J. Ma, S. R. Kass, *J. Org. Chem.* **2019**, 84, 11125.
- [12] A *para*-N-alkylated thiourea has been studied (see ref. 10d) and phosphonium phosphoric acids have been reported (see refs. 11b and 11c).
- [13] a) T. Schuster, M. Kurz, M. W. Gobel, *J. Org. Chem.* **2000**, 65, 1697. b) D. Akalay, G. Durner, J. W. Bats, M. Bolte, M. W. Gobel, *J. Org. Chem.* **2007**, 72, 5618.
- [14] a) E. J. Corey, M. J. Grogan, *Org. Lett.* **1999**, 1, 157. b) M. Terada, H. Ube, Y. Yaguchi, *J. Am. Chem. Soc.* **2006**, 128, 1454. c) M. Terada, M. Nakano, H. Ube, *J. Am. Chem. Soc.* **2006**, 128, 16044. d) C. Uyeda, E. N. Jacobsen, *J. Am. Chem. Soc.* **2008**, 130, 9228. e) D. Leow, C.-H. Tan, *Synlett* **2010**, 2010, 1589. f) C. Uyeda, E. N. Jacobsen, *J. Am. Chem. Soc.* **2011**, 133, 5062. g) P. Selig, *Synthesis* **2013**, 45, 703. (h) M. P. Coles, *Chem. Commun.* **2009**, 25, 3659.
- [15] J. Huang, E. J. Corey, *Org. Lett.* **2004**, 6, 5027.
- [16] a) N. Takenaka, R. S. Sarangthem, S. K. Seerla, *Org. Lett.* **2007**, 9, 2819. b) N. Takenaka, J. Chen, B. Captain, R. S. Sarangthem, A. Chandrakumar, *J. Am. Chem. Soc.* **2010**, 132, 4536. c) Y. Nishikawa, S. Nakano, Y. Tahira, K. Terazawa, K. Yamazaki, C. Kitamura, O. Hara, *Org. Lett.* **2016**, 18, 2004.
- [17] a) B. M. Nugent, R. A. Yoder, J. N. Johnston, *J. Am. Chem. Soc.* **2004**, 126, 3418. b) A. Singh, R. A. Yoder, B. Shen, J. N. Johnston, *J. Am. Chem. Soc.* **2007**, 129, 3466. c) A. Singh, J. N. Johnston, *J. Am. Chem. Soc.* **2008**, 130, 5866. d) M. Ganesh, D. Seidel, *J. Am. Chem. Soc.* **2008**, 130, 16464.
- [18] C. Bolm, T. Rantanen, I. Schiffrers, L. Zani, *Angew. Chem. Int. Ed.* **2005**, 44, 1758.
- [19] L. A. Curtiss, P. C. Redfern, K. Raghavachari, *J. Chem. Phys.* **2007**, 126, 084108.
- [20] N. A. Yakelis, R. G. Bergman, *Organometallics* **2005**, 24, 3579.
- [21] D. R. Burfield, R. H. Smithers, A. S. C. Tan, *J. Org. Chem.* **1981**, 46, 629.
- [22] C. P. Rosenau, B. J. Jelner, A. D. Gossert, A. Togni, *Angew. Chem. Int. Ed.* **2018**, 57, 9528.
- [23] a) P. Beak, J. Bonham, *J. Am. Chem. Soc.* **1965**, 87, 3365. b) A. R. Katritzky, R. C. Patel, M. Shanta, *J. Chem. Soc., Perkin Trans. 1* **1980**, 11, 1888. c) P. Guerry, R. Neier, *Synthesis* **1984**, 1984, 485.

- [24] This is given as a septet rather than a triplet based upon its chemical assignment, despite the fact that not all of the peaks are fully resolved.
- [25] P. J. Stang, G. Maas, D. L. Smith, J. A. McCloskey, *J. Am. Chem. Soc.* **1981**, 103, 4837.
- [26] This is given as a septet rather than a pentet based upon the chemical assignment and the observed intensities even though the outermost peaks are not visible. That is, the five lines better fit to a 1:2.5:3.3:2.5:1 ratio rather than a 1:4:6:4:1 distribution.
- [27] C. Yin, K. Zhong, W. Li, X. Yang, R. Sun, C. Zhang, X. Zheng, M. Yuan, R. Li, Y. Lan, H. Fu, H. Chen, *Adv. Synth. Catal.* **2018**, 360, 3990.
- [28] J. Mendez-Arroyo, J. Barroso-Flores, A. M. Lifschitz, A. A. Sarjeant, C. L. Stern, C. A. Mirkin, *J. Am. Chem. Soc.* **2014**, 136, 10340.
- [29] F. J. Arnaiz, *J. Chem. Educ.* **1995**, 72, 1139.
- [30] C. M. McGuirk, J. Mendez-Arroyo, A. I. d'Aquino, C. L. Stern, Y. Liu, C. A. Mirkin, *Chem. Sci.* **2016**, 7, 6674.
- [31] This feature is comprised of a triplet (8.67, 1H) overlapping with a doublet (8.65, 1H).
- [32] a) A. D. Becke, *J. Chem. Phys.* **1993**, 98, 5648. b) C. Lee, W. Yang, R. G. Parr, *Phys. Rev. B* **1988**, 37, 785.
- [33] a) Y. Zhao, D. G. Truhlar, *J. Phys. Chem. A* **2008**, 112, 1095. b) Y. Zhao, D. G. Truhlar, *Theor. Chem. Account* **2008**, 120, 215. c) Y. Zhao, D. G. Truhlar, *Acc. Chem. Res.* **2008**, 41, 157.
- [34] M. J. Frisch, G. W. Trucks, H. B. Schlegel, G. E. Scuseria, M. A. Robb, J. R. Cheeseman, G. Scalmani, V. Barone, G. A. Petersson, H. Nakatsuji, X. Li, M. Caricato, A. V. Marenich, J. Bloino, B. G. Janesko, R. Gomperts, B. Mennucci, H. P. Hratchian, J. V. Ortiz, A. F. Izmaylov, J. L. Sonnenberg, D. Williams-Young, F. Ding, F. Lipparini, F. Egidi, J. Goings, B. Peng, A. Petrone, T. Henderson, D. Ranasinghe, V. G. Zakrzewski, J. Gao, N. Rega, G. Zheng, W. Liang, M. Hada, M. Ehara, K. Toyota, R. Fukuda, J. Hasegawa, M. Ishida, T. Nakajima, Y. Honda, O. Kitao, H. Nakai, T. Vreven, K. Throssell, J. A. Montgomery Jr., J. E. Peralta, F. Ogliaro, M. J. Bearpark, J. J. Heyd, E. N. Brothers, K. N. Kudin, V. N. Staroverov, T. A. Keith, R. Kobayashi, J. Normand, K. Raghavachari, A. P. Rendell, J. C. Burant, S. S. Iyengar, J. Tomasi, M. Cossi, J. M. Millam, M. Klene, C. Adamo, R. Cammi, J. W. Ochterski, R. L. Martin, K. Morokuma, O. Farkas, J. B. Foresman, D. J. Fox, *Gaussian 16*, Gaussian, Inc, Wallingford CT **2016**.
- [35] GaussView, Version 6, R. Dennington, T. Keith, J. Millam, Semicem Inc., Shawnee Mission, KS, **2016**.
- [36] A similar procedure has been used before, see ref. 9.
- [37] For some reports regarding the tautomeric equilibria of 2- and 4-hydroxypyridines, see a) J. Wang, R. J. Boyd, *J. Phys. Chem.* **1996**, 100, 16141. b) L. Forlani, G. Cristoni, C. Boga, P. E. Todesco, E. Del Vecchio, S. Selva, M. Monari, *ARKIVOC* **2002**, 11, 198. c) J. Gao, L. Shao, *J. Phys. Chem.* **1994**, 98, 13772. d) P. Beak, J. B. Covington, S. G. Smith, J. M. White, J. M. Zeigler, *J. Org. Chem.* **1980**, 45, 1354. e) N. Tsuchida, S. Yamabe, *J. Phys. Chem. A* **2005**, 109, 1974.
- [38] For some examples of *N*- and *O*- alkylation studies of 2- and 4-hydroxypyridines and related compounds, see a) F. You, R. J. Twieg, *Tetrahedron Lett.* **1999**, 40, 8759. b) M. Breugst, H. Mayr, *J. Am. Chem. Soc.* **2010**, 132, 15380. c) D. L. Comins, G. Jianhua, *Tetrahedron Lett.* **1994**, 35, 2819. d) O. R. Ludek, C. Meier, *Synlett* **2006**, 2006, 324. e) M. Torres, S. Gil, M. Parra, *Curr. Org. Chem.* **2005**, 9, 1757. f) H. Liu, S. B. Ko, H. Josien, D. P. Curran, *Tetrahedron Lett.* **1995**, 36, 8917. g) T. Sato, K. Yoshimatsu, J. Otera, *Synlett* **1995**, 1995, 845.
- [39] J. E. Bartmess, *NIST Chemistry WebBook, NIST Standard Reference Database Number 6*; W. G. Mallard, P. J. Lustrum, National Institute of Standards and Technology: Gaithersburg, MD (<http://webbook.nist.gov>).
- [40] This trend was observed in our initial study (ref. 9) but the range of the free O–H frequencies was only ~20 cm<sup>-1</sup> for 20 substituted phenols.
- [41] See Supporting Information for titration plots for all compounds in this work.
- [42] See Supporting Information for pictures of titrant solutions.
- [43] The  $\alpha$ -carbon hydrogen bonds of tetraalkylammonium salts have been reported to participate in hydrogen bonding, see a) Y. Kumatabara, S. Kaneko, S. Nakata, S. Shirakawa, K. Maruoka, *Chem. Asian J.* **2016**, 11, 2126. b) S. Shirakawa, S. Liu, S. Kaneko, Y. Kumatabara, A. Fukuda, Y. Omargari, K. Maruoka, *Angew. Chem. Int. Ed.* **2015**, 54, 15767. c) T. C. Cook, M. B. Andrus, D. H. Ess, *Org. Lett.* **2012**, 14, 5836. d) C. E. Cannizzaro, K. N. Houk, *J. Am. Chem. Soc.* **2002**, 124, 7163. Also, see e) C. T. Dewberry, J. L. Mueller, R. B. Mackenzie, B. A. Timp, M. D. Marshall, H. O. Leung, K. R. Leopold, *J. Mol. Struct.* **2017**, 1146, 373. and refs. therein
- [44] a) P. Thordarson, *Chem. Soc. Rev.* **2011**, 40, 1305. b) B. D. Hibbert, P. Thordarson, *Chem. Commun.* **2016**, 52, 12792. c) See also [supramolecular.org](http://supramolecular.org).
- [45] F. Ulatowski, K. Dabrowa, T. Balakier, J. Jurczak, *J. Org. Chem.* **2016**, 81, 1746.
- [46] A monomer/dimer equilibrium process was not included in binding isotherm fits, but modifying the initial concentrations of **4H** accordingly has no effect on the resulting association constants. This is because at the employed concentrations for the titrations, the dimer contribution is negligible (<< 0.01%).
- [47] For the kinetic data, see Supporting Information.
- [48] This compound was also employed in the UV-vis titration with **1**. See the Supporting Information for more details.
- [49] Under the reaction conditions, >99% of **2MeOPyrH** is in the monomeric form. For the dimerization data, see Supporting Information.

## SUPPORTING INFORMATION

Additional supporting information may be found online in the Supporting Information section at the end of this article.

**How to cite this article:** Payne C, Kass SR. Structural considerations for charge-enhanced Brønsted acid catalysts. *J Phys Org Chem.* 2020; e4069. <https://doi.org/10.1002/poc.4069>